



# Impacts of degrading permafrost on streamflow in the source area of Yellow River on the Qinghai-Tibet Plateau, China

MA Qiang<sup>a,b</sup>, JIN Hui-Jun<sup>a,c,\*</sup>, Victor F. BENSE<sup>a,d</sup>, LUO Dong-Liang<sup>a</sup>,  
Sergey S. MARCHENKO<sup>e</sup>, Stuart A. HARRIS<sup>f</sup>, LAN Yong-Chao<sup>a</sup>

<sup>a</sup> State Key Laboratory of Frozen Soils Engineering, Northwest Institute of Eco-Environment and Resources, Chinese Academy of Sciences, Lanzhou, 730000, China

<sup>b</sup> College of Resources and Environment, University of Chinese Academy of Sciences, Beijing, 100049, China

<sup>c</sup> School of Civil Engineering, Harbin Institute of Technology, Harbin, 150090, China

<sup>d</sup> Hydrology and Quantitative Water Management Group, Department of Environmental Sciences, Wageningen University, Wageningen, 6708PB, the Netherlands

<sup>e</sup> Geophysical Institute (GIPL), University of Alaska Fairbanks, Fairbanks, 99775, USA

<sup>f</sup> Department of Geography, University of Calgary, Calgary, T3A 1E4, Canada

Received 14 November 2019; revised 13 January 2020; accepted 8 February 2020

## Abstract

Many observations in and model simulations for northern basins have confirmed an increased streamflow from degrading permafrost, while the streamflow has declined in the source area of the Yellow River (SAYR, above the Tanag hydrological station) on the northeastern Qinghai-Tibet Plateau, West China. How and to what extent does the degrading permafrost change the flow in the SAYR? According to seasonal regimes of hydrological processes, the SAYR is divided into four sub-basins with varied permafrost extents to detect impacts of permafrost degradation on the Yellow River streamflow. Results show that permafrost degradation may have released appreciable meltwater for recharging groundwater. The potential release rate of ground-ice melt-water in the Sub-basin 1 (the headwater area of the Yellow River (HAYR), above the Huangheyan hydrological station) is the highest (5.6 mm per year), contributing to 14.4% of the annual Yellow River streamflow at Huangheyan. Seasonal/intra- and annual shifts of streamflow, a possible signal for the marked alteration of hydrological processes by permafrost degradation, is observed in the HAYR, but the shifts are minor in other sub-basins in the SAYR. Improved hydraulic connectivity is expected to occur during and after certain degrees of permafrost degradation. Direct impacts of permafrost degradation on the annual Yellow River streamflow in the SAYR at Tanag, i.e., from the meltwater of ground-ice, is estimated at 4.9% that of the annual Yellow River discharge at Tanag, yet with a high uncertainty, due to neglecting of the improved hydraulic connections from permafrost degradation and the flow generation conditions for the ground-ice meltwater. Enhanced evapotranspiration, substantial weakening of the Southwest China Autumn Rain, and anthropogenic disturbances may largely account for the declined streamflow in the SAYR.

**Keywords:** Streamflow; Warming climate; Permafrost degradation; Streamflow patterns; Source area of Yellow River (SAYR)

## 1. Introduction

Many recent studies have reported an increased streamflow due to degrading permafrost in northern basins (e.g., Ge et al., 2013; Bring and Destouni, 2014; Haine et al., 2015; Bring et al., 2016, 2017; Kurylyk et al., 2016), as well as many permafrost basins on the Qinghai-Tibet Plateau (QTP) (e.g., Ye et al., 2012; Han et al., 2016; Gao et al., 2018; Wang et al.,

\* Corresponding author. State Key Laboratory of Frozen Soils Engineering, Northwest Institute of Eco-Environment and Resources, Chinese Academy of Sciences, Lanzhou, 730000, China.

E-mail address: [hjjin@lzb.ac.cn](mailto:hjjin@lzb.ac.cn) (JIN H.-J.).

Peer review under responsibility of National Climate Center (China Meteorological Administration).

<https://doi.org/10.1016/j.accre.2020.02.001>

1674-9278/Copyright © 2020, National Climate Center (China Meteorological Administration). Production and hosting by Elsevier B.V. on behalf of KeAi. This is an open access article under the CC BY-NC-ND license (<http://creativecommons.org/licenses/by-nc-nd/4.0/>).

2018a; Xu et al., 2019). However, in the source area of the Yellow River (YR) (SAYR, above Tanag (TNG), Qinghai province, West China), with a widespread presence of discontinuous, sporadic and patchy permafrost and seasonal frost (Jin et al., 2009), which are vulnerable to climate warming. A declined streamflow has been detected in spite of a slightly increasing precipitation (0.3 mm per year) during 1961–2017.

Since 1976, annual mean air temperature (AMAT) in the SAYR has been increasing rapidly (0.39 °C per decade), almost twice as rapidly as the global average warming rate (0.2 °C per decade) (IPCC, 2013). The SAYR has also undergone significant climate warming, which is greater than some other sub-regions on the QTP (Cheng et al., 2019). Borehole data and observations also show progressive ground warming (0.19 °C per year) in 2010–2016 at Xingxinghai in the upstream SAYR (Luo et al., 2018). Elevation of the lower limit of permafrost (e.g., 4320–4370 m a.s.l. at Yeniugou on the northern slope of the Bayan Har Mountains) (Jin et al., 2009), shrinkage of the areal extent of permafrost, and declined maximum depth of seasonal frost penetration (3.5 cm per decade) (Qin et al., 2017; Luo et al., 2018; Wang et al., 2018b; Zheng et al., 2019) are frequently reported in the SAYR above TNG.

The SAYR, one of the key Asian Water Towers, covering a catchment area of 16.2% of the Yellow River Basin ( $752.4 \times 10^3 \text{ km}^2$ ), but providing about 54.7% ( $20.0 \times 10^9 \text{ m}^3$  at the TNG) of the multi-year average of annual discharge ( $36.5 \times 10^9 \text{ m}^3$  at the Lijin hydrological station in Shandong province, East China) of the Yellow River to the Pacific Ocean (CMWR, 2008–2017), is disproportionately important for the basin-wide YR flow regimes. Decreasing surface water resources and three recorded dry-ups of YR streamflow in the upstream SAYR in 1980, 1988 and 1995 have caused extensive and intense concerns in China and abroad.

Because of intricate nature of changing trends and mechanisms of flow regimes in cold regions, some recent research have tried in revealing, quantifying, or attributing the impacts of permafrost degradation on/to the decreased YR flows (e.g., Lan et al., 2015; Niu et al., 2016; Xu et al., 2016; Wang et al., 2017, 2018c, 2018d; Wu et al., 2018). They have explored the impacts of permafrost degradation on the YR discharge by methods of identifying the increase in groundwater storage (e.g., Niu et al., 2016; Xu et al., 2016; Wang et al., 2017), or mathematical model simulations to decompose the streamflow components (e.g., Budyko framework or mathematical model) (Wang et al., 2018c; Wu et al., 2018). Employing a process-based Variable Infiltration Capacity model, Lan et al. (2015) tried in explaining the effect of degrading permafrost on surface hydrology. Yet, conclusions are mixed and mostly derived from relationship analysis for water-balance items. The impacting mechanisms of degrading permafrost on hydrological processes are hardly examined. The questions as how, and to what extent, permafrost degradation would alter the streamflow regimes in the SAYR, remain unanswered.

In this study, we discuss the mechanisms for hydrological impacts of permafrost degradation and quantitatively examine major impacting mechanisms for the YR streamflow with accessible and reliable long-term observational data. Knowledge of seasonal regimes in hydrology is applied and season is re-divided according to the hydrogeological and hydrological features of the SAYR catchment. Corrections of precipitation, evaporation and YR streamflow are made for obtaining the actual values of water-balance components. Focusing on the hydrological impacts, on the YR streamflows in particular, from degrading permafrost, these studies are key to understanding the water cycles and water resources in the upper Yellow River Basin and important for water supply and safety in the YR Basin.

## 2. Study regions

The SAYR, i.e., the catchment of the Yellow River (YR) Basin above TNG (32°10′–36°7′N, 95°54′–103°24′E; 2629–6253 m a.s.l.) on the northeastern QTP, has a catchment area of 120,900 km<sup>2</sup>. For comparison, the SAYR is divided into four sub-basins with varied permafrost extents and other basin characteristics by four major hydrological stations on the YR mainstream as follows: Sub-basin 1 (the headwater area of the Yellow River (HAYR), above Huangheyan hydrological station, abbreviated as HHY), Sub-basin 2 (between HHY and Jimai (JM)), Sub-basin 3 (between JM and Maqū (MQ)), and Sub-basin 4 (between MQ and TNG) (Fig. 1). The landscape of the SAYR is characterized by low-relief valleys surrounded by high mountains, as a result of collision of the India Plate with the Asia Plate, forming extensive strike-slip and normal faults (Lutgens and Tarbuck, 2012). Due to the low-relief valleys, stream channels in the Sub-basin 1 (HAYR) are largely braided and meandering (Jin et al., 2009). The Sub-basin 2 enters high-relief gorges of the A'nyëmaqên Mountains, where stream channels are deeply incised. In the Sub-basin 3, a knickpoint induces an abrupt loss of streamflow momentum and change its flow direction, forming meandering rivers and tributaries and numerous paleo-river channels on the Zoïgé Plateau. In the Sub-basin 4, stream channels are deeply cut and laterally constrained. Due to extensive glaciations, wind and river processes since the Pleistocene, fluvial-alluvial, aeolian and glacio-lacustrine sediments are widely deposited in the SAYR (Blue et al., 2013).

Only 166 contemporary glaciers present at elevations of 4400–6000 m a.s.l. in the A'nyëmaqên Mountains, with an areal extent of ~126.7 km<sup>2</sup>, and; glacier-melt contributes only 1%–2% of annual discharge at TNG (Blue et al., 2013; Jin et al., 2019). Alpine meadows and steppes prevail in the HAYR. In lower catchments, shrubs and forests start to appear in patches. The Zoïgé Plateau in the Sub-basin 3 is characterized by extensive occurrences of wetlands and aquatic vegetation, with peat layers as deep as 5.0–10.5 m in some areas. Along the southeastward declining elevational and climate gradients, discontinuous, sporadic and patchy permafrost and seasonal frost occur cascadingly downwards. Influenced by regional

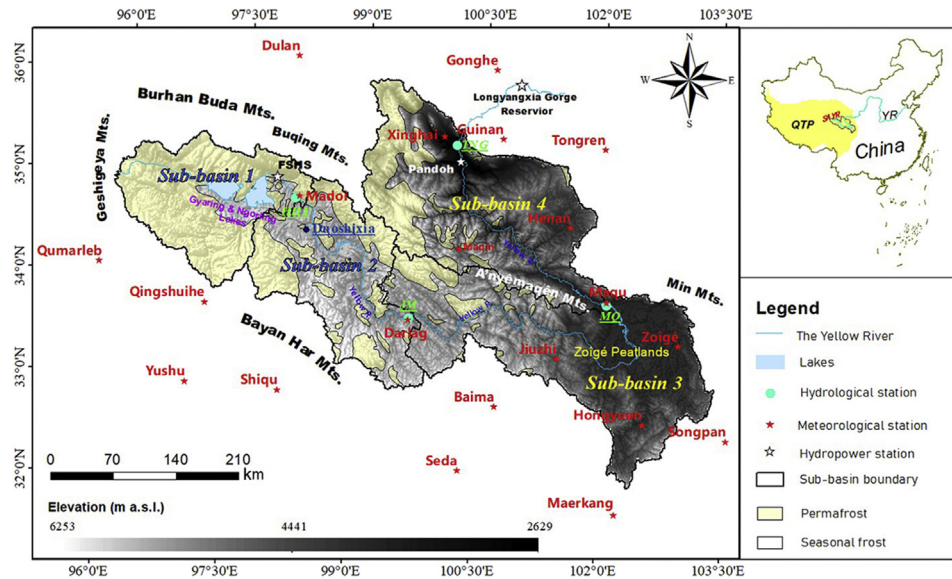


Fig. 1. Sub-basin division in the source area of the Yellow River (SAYR), northeastern Qinghai-Tibet Plateau, West China.

and local climate conditions, the relatively humid climate in southern and eastern SAYR results in more ice-rich permafrost and widespread wetlands, while it is more arid in northern SAYR, with widespread occurrences of mobile sand dunes and sand-lands (Blue et al., 2013).

In 1998–2003, the First SAYR hydropower station (FSHS, also called the Ngöring Lake Reservoir), was built for Madoi county town in the Sub-basin 1 (HAYR). In 2007, the Pandoh hydropower station was built in the Sub-basin 4 and subsequently put to operation (Fig. 1). Additionally, in the Sub-basin 4, some smaller dams, as Moduo, Dancun and Gaqu dams (Fig. 1), were also built for power generation, domestic usage and irrigation. These reservoirs alter spatial and temporal distributive features of the YR streamflows and promote domestic usage and agricultural irrigation, subsequently reducing the YR streamflow. More detailed information is presented in Table 1.

### 3. Materials and methods

#### 3.1. Data acquisition

The data of monthly YR streamflow in the SAYR are collected at the above mentioned four hydrological stations (HHY, JM, MQ and TNG). Thus, the YR streamflow generated in each sub-basin is obtained by subtracting the streamflow at the last upstream hydrological station from that at the control station in this sub-basin. Data for daily temperature, precipitation, wind speed and evaporation (20-cm-pan) are downloaded from the National Meteorological Information Center of China Meteorological Administration (<http://data.cma.cn>). The period of meteorological data extended for 57 hydrological years from November 1961 to October 2017. A hydrological year is set from November to the next October on the basis of regimes in monthly average air temperature,

precipitation and flow. Yearly data here all refer to those hydrological years. Areal extent of permafrost is extracted from Ran et al. (2012) and/or Brown et al. (2002). Permafrost thickness and ground temperature data are from *in-situ* borehole monitoring. Digital elevation model (DEM) is downloaded from <https://earthexplorer.usgs.gov/> and hydrology module in ArcGIS is employed to obtain the basin boundary.

#### 3.2. Analytical methods

The hydrological data in the SAYR were validated by employing the method of Double Mass Curve (DMC) (Searcy and Hardison, 1960). In this method, data are reformatted by adding all data up before this datum in time series of control and validated stations. Then, the reformatted data are plotted as x- or y-coordinates.

Daily precipitation data are measured by Chinese standard precipitation gauge (CSPG) for measuring liquid and solid precipitation at national meteorological stations. A systematic error occurs by employing CSPG, especially in cold environments (Ye et al., 2004; Yang et al., 2005). Wetting loss, evaporation loss, and trace precipitation and wind-induced gauge under-catch are taken into account of when validating daily precipitation data in the SAYR according to Ye et al. (2004).

It is found the annual evaporation data of 20-cm pan measured at meteorological stations in the SAYR are about 2.5 times larger than the estimated actual evaporation by Gravity Recovery and Climate Experiment (GRACE) satellite data and intra-annual variability differs between these two evaporation datasets (Xu et al., 2013). The inter- and intra-annual variability of evaporation among four sub-basins is similar and modulated according to the estimated actual evaporation by GRACE. Inter-monthly, -seasonal and -annual trends of major hydrometeorological variables in each sub-basin and in the SAYR were obtained by linear regression analysis.

Table 1  
Climate, geomorphology, permafrost and vegetation characteristics in four sub-basins in the source area of Yellow River (SAYR) on northeastern Qinghai-Tibet Plateau.

Character	Sub-basin 1 (HAYR)	Sub-basin 2	Sub-basin 3	Sub-basin 4	SAYR
Region	Above HHY	HHY-JM	JM-MQ	MQ-TNG	Above TNG
Sub-basin area (10 <sup>3</sup> km <sup>2</sup> )	21.0	23.6	39.7	36.6	120.9
Areal percentage in SAYR (%)	17.4	19.5	32.8	30.3	100.0
Elevation (m a.s.l.)	4207–5245	3942–5354	3406–5335	2629–6253	2629–6253
Dominant geomorphology	High mountains and low-relief valleys	Mainly narrow gorges	Narrow gorges and Zoigé Plateau	Mainly narrow gorges	High mountains, low-relief valleys and narrow gorges
Vegetation types	Alpine steppes and meadow	Alpine steppes and coniferous forests	Aquatic vegetation, shrubs, broad-leaf forests	Shrubs and broad-leaf forests	Alpine meadow and steppes in upstreams; aquatic vegetation, shrubs, forests in lower reaches
Soil types	Dark calcareous soil, calcareous soil, Alpine meadow soil	Dark calcareous soil and alpine meadow soil	Black felted soil, boggy soil and alpine meadow soil	Alpine meadow soil, thin vegetation mat soil, thin black felt soil and light calcareous soil	Dominated by alpine meadow soil, widespread calcareous and dark calcareous soil in upstream. More boggy soil and black felt soil on the Zoigé Plateau
Topography and drainage	Meandering rivers	Constrained rivers	Mixture of constrained and braided rivers	Constrained rivers	Mixture of constrained and meandering rivers
Major human activities for hydrological impacts	Damming and grazing	Grazing	Grazing, drainage for corplands	Damming, drainage for corplands and grazing	Generally minimal human disturbances. More human activities in downstream
Permafrost coverage (%)	86	42	9	27	34
Frozen ground type	Discont to sporadic permafrost	Sporadic permafrost to seasonal permafrost	Sporadic permafrost to seasonal permafrost	Discontinuous to sporadic permafrost and seasonal permafrost	
Annual mean ground temperature (°C) <sup>a</sup>	–3.5–0	–3.5–0	–3.5–0	–3.5–0	–3.5–0
Measured/estimated permafrost thickness (m) <sup>b</sup>	0–176	0–224	0–176	0–516	0–516
Annual precipitation (mm)	484–755	500–849	695–1021	424–882	424–1021
Mean January precipitation (mm)	19.7–22.4	19.4–22.7	18.1–21.4	16.4–20.6	16.4–22.7
Mean July precipitation (mm)	93–132	97–149	121–157	66–150	66–157
Annual mean air temperature (°C)	–4.4 to –0.7	–3.5–2.0	–1.3–7.5	–1.8–3.3	–4.4–7.5
Mean January air temperature (°C)	–14 to –12.3	–14.1 to –11.7	–12.9 to –6.9	–12.7 to –9.2	–14.1 to –6.9
Mean July air temperature (°C)	8.3–10.3	8.3–10.2	9.4–13.9	10–13.4	8.3–13.9
Climate and permafrost features	Large permafrost extent and cold-dry climate	Moderate permafrost coverage, wet-cold	Small permafrost extent, warm-wet	Moderate permafrost coverage and warm-dry climate	Wide-spread discont permafrost and seasonal frost; arid climate in Northwest and wet in Southeast, cold in upstreams and warm in downstreams

Notes: Climate data are for the period of 1961–2017; <sup>a</sup>Wang and French (1995); <sup>b</sup>Wang and French (1994), Jin et al. (2009).

### 3.3. Seasonal division in sub-basins

Hydrological processes are strongly featured by seasonality. In winter when everything on ground surface is immobilized by cold weather, ground freezing and snow cover, streamflow in permafrost regions are mainly recharged by

groundwater (Woo, 2012). In spring, snow cover begins to melt and the snow-melting is accompanied by intermittent spring snowfall and/or rainfall, and streamflow gradually picks up. The spring streamflow is mainly correlated to winter and spring precipitation input and near-surface hydrological processes (Woo, 2000; Neff et al., 2006). In summer and autumn,

high precipitation input dominates the streamflow, which depends on the balance between evaporation and rainfall (Carey and Woo, 2001a, 2001b). However, the common division of four seasons appears unreasonable for alpine and Arctic regions since different watersheds have a varied duration of hydrological seasons (Takeuchi et al., 2004; Yang et al., 2009; Ye et al., 2009).

By taking into account of features in multi-year averages of mean monthly air temperatures, precipitation and streamflow in each sub-basin of the SAYR, it is found that precipitation largely synchronizes with air temperature. In the HAYR (the highest and coldest sub-basin in the SAYR), the period of subzero monthly mean air temperature (MMAT) occurs from November to April in comparison with the period of November to March in other three sub-basins. In the subsequent two months (May–June for the HAYR and April–May for Sub-basins 2, 3, and 4), MMAT turns above zero and the YR streamflow keeps low, but shows a slight pickup. In summer and autumn, MMAT goes the highest in the year and precipitation and streamflow peaks largely correspond to rainstorms. Despite of different duration of seasons between the HAYR and other sub-basins, shifts in streamflow in each season and their responses to changes in precipitation and evaporation are detectable in each sub-basin. The hydrological seasons are thus divided as follows:

- 1) Winter season (November to next April in the HAYR, and November to next March in Sub-basins 2, 3, and 4) captures the low streamflow and subzero MMAT.
- 2) Spring season is from May to June in the HAYR and from April to May in Sub-basins 2, 3 and 4. Air temperature begins to go above 0 °C. The snow cover in winter starts to melt, and occasional rainfall may initiate near-surface hydrological processes with increasing thaw depth.
- 3) Summer season (July–August in the HAYR; June–August in Sub-basins 2, 3 and 4) captures the large amount of precipitation and higher temperatures in

a year. In summer, rainstorms dominate in-stream streamflow.

- 4) Autumn season (September–October) captures the similar hydrological processes as summer season. A second peak rainfall (in autumn) in a year is well-known in China as Southwest China Autumn Rain (Bai and Dong, 2004).

### 3.4. Flow data validation

Except for actual evaporation and precipitation, reliable streamflow data are critical for analyzing the impacts of permafrost degradation on the YR streamflow in the SAYR. Zhang et al. (2004) found close relationships among the streamflow data at four hydrological stations in the SAYR and the DMC analysis revealed a particular inclination among four hydrological stations. Fig. 2 indicates that, since 1998, the construction of the FSHS has largely altered the YR streamflow at HHY.

Since January 1998 when the FSHS began to build, the DMC started to go downwards due to the damming of stream channel for construction work. The FSHS was put to operation in February 2000 and the curve went upward for a short period (February 2000 to December 2002). Then, the FSHS stopped functioning from January 2003 to June 2005, due to the abnormally low flow, or dry-up. During these periods, the uncorrected cumulative curve went much smoother, almost horizontal, due to continuous impoundment of water in the reservoir.

The FSHS was again put back to operation in June 2005. Since 2007, precipitation began to increase notably and incoming water to the reservoir was mostly discharged. During the period between January 2007 and September 2016, there was a trend for the YR discharge to return to its original inclination before January 1998. Since October 2016, the State Grid has been supplying electricity for Madoi county town and the power generation of the FSHS has been

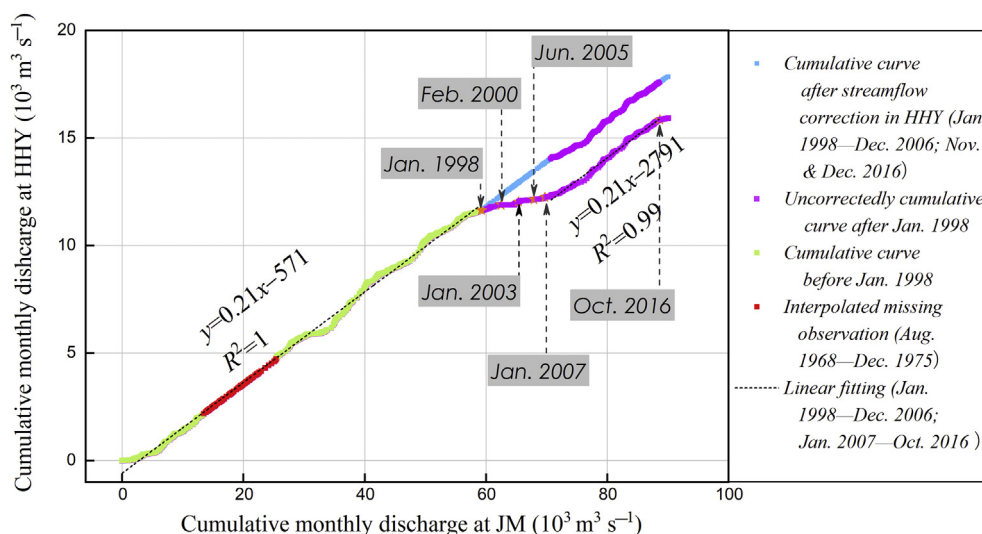


Fig. 2. Double mass curve (DMC) between the Huangheyuan (HHY) and Jima (JM) hydrological stations for correcting the Yellow River (YR) discharge at HHY near Madoi, Qinghai province on the northeastern Qinghai-Tibet Plateau.

suspended. As a result, inclination of cumulative curve has gone smooth again. Thus, in wetter years, the FSHS, with only a limited storage capacity, discharges most incoming water. However, in drier years, the reservoir management prefers to the impoundment of water, and smaller-than-normal streamflows are measured.

The streamflow data at HHY are corrected for the period since the construction of the FSHS dam (January 1998) to the turning point of returning to its original inclination (January 2007) and the period between October 2016 and October 2017 (in blue color). The FSHS is planned to be totally dismantled due to the eco-environmental concerns and as a partial effort of establishing the Three-Rivers Source Area National Park of China. The removal of the dam may help the cumulative DMC curve restore to its original shape.

#### 4. Effect of permafrost degradation on YR streamflow in the SAYR

##### 4.1. Melting ground ice

The melting of excess-ice in permafrost soils may release a certain amount of meltwater in favorable flow-generation environments (O'Donnell et al., 2016). Wang et al. (2018a) roughly estimated the average volumetric ice content of permafrost in the SAYR above Duoshixia (34°34'42"N, 98°19'24"E; 4197 m a.s.l.) at  $0.31 \pm 0.11 \text{ m}^3 \text{ m}^{-3}$ . This can be employed as the average for that of the SAYR because the major portion of permafrost in the SAYR is found above Duoshixia. Wang et al. (2018b) projected that most of the permafrost in the SAYR would thaw by 2100 under the RCP 4.5 scenario. Thus, the potential average release rate of ground-ice meltwater was roughly estimated by Eq. (1), due to the data gap for accurate estimation of ground-ice meltwater in the SAYR:

$$R_{\text{im}} = 1000 \times (PA \times C \times D \times C_{\text{ice}}) / (CA \times T) \quad (1)$$

where  $R_{\text{im}}$  is the average release rate of ground-ice meltwater in mm per year;  $PA$  is permafrost area in  $\text{km}^2$ ;  $C$  is the areal continuity of different permafrost types (continuous permafrost: 0.95, discontinuous permafrost: 0.7, sporadic permafrost: 0.3, isolated patches of permafrost: 0.05) (Brown et al., 2002), dimensionless;  $D$  is the thickness of permafrost with ground ice occurrence in m;  $C_{\text{ice}}$  is average volumetric ice content at the given depth range in  $\text{m}^3 \text{ m}^{-3}$ ;  $CA$  is catchment area in  $\text{km}^2$ , and;  $T$  is projected time span of permafrost disappearance in year.

The potential average release rate of ground-ice meltwater is 2.2 mm per year, which is relatively small in comparison

with the YR streamflow depth of 167 mm per year in the SAYR (1961–2017). The potential ground-ice melt-water from the Sub-basin 1 (HAYR) is the highest, accounting for 14.4% to the YR streamflow at HHY, in comparison with this proportion of less than 2% in other three sub-basins (Table 2). However, this estimation is of large uncertainty, due to the fact that, in general, only the melting of excess ice in permafrost soils could generate runoff at favorable flow-generation environments. Meanwhile, the projected time span of disappearance of permafrost is also highly uncertain.

In northern regions, especially in coastal lowlands in northern parts of Siberia, Alaska, Canada and Europe, permafrost is continuous and icy. Reported volumetric ground-ice content can be as high as  $0.4\text{--}0.6 \text{ m}^3 \text{ m}^{-3}$ , and that of ice-wedge complexes (yedoma),  $>0.9 \text{ m}^3 \text{ m}^{-3}$  (Fritz et al., 2015). Kokelj et al. (2013) reported that thawing of massive ground-ice in permafrost catchments in northwestern Canada could cause large diurnal fluctuations (one order of magnitude) in streamflows. Scheidegger (2013) highlighted increasing streamflow and baseflow discharge to the Arctic Ocean. St. Jacques and Sauchyn (2009) noted the association of the increased streamflow with changes in permafrost thickness and extent. Lan et al. (2015) also found a positive relationship between increasing moisture contents of deep soil and baseflow in catchments with degrading permafrost on the northern QTP, implying a possible contribution to groundwater storage from thawing permafrost.

Thus, even though direct evidence can hardly be provided so far in the SAYR, an increased ground-ice melt-water discharge into groundwater has been extensively detected in the North (e.g., St. Jacques and Sauchyn, 2009; Kokelj et al., 2013; Scheidegger, 2013) and in some other regions on the QTP (e.g., Lan et al., 2015; Niu et al., 2016; Xu et al., 2016; Wang et al., 2017). This indirectly proves ice-melt will potentially increase groundwater storage in the SAYR. The recharging rate by potential ice-melt in the Sub-basin 1 (HAYR), with an areal extent of permafrost at 86%, can be as high as 14.4% and; that is 1.3% in the SAYR, with an average areal extent of permafrost at 34%.

##### 4.2. Improved hydraulic connections

Thermokarst lakes, icings, springs and pingos in permafrost regions are commonly related with discharge of the sub-permafrost water. As an aquitard, permafrost largely confines the sub-permafrost water and produces a high artesian water-head. The sub- or intra-permafrost water can be delivered to the ground surface through open-taliks, generally in association with active faults. Thus, with permafrost

Table 2  
Comparison of potential release rates of ground-ice meltwater and streamflow depth in sub-basins in the SAYR on the northeastern Qinghai-Tibet Plateau.

Hydrological parameters	Sub-basin 1	Sub-basin 2	Sub-basin 3	Sub-basin 4	SAYR
Potential release rate of ground-ice meltwater (mm per year)	5.6	2.7	0.6	1.8	2.2
YR streamflow depth (mm per year)	39.0	140.0	256.0	161.0	167.0
Contribution ratio of potential ground-ice meltwater to the YR streamflow (%)	14.4	1.9	0.2	1.1	1.3

degradation, a better hydraulic connection will alter or modify streamflow dynamics.

Numerous springs and icings have been found in a continuous-permafrost catchment in northeastern Alaska, with the sub-permafrost aquifers identified as the recharging source (e.g., Kane et al., 2013). Thermokarst or other types of lakes can drain through open-talik as well. Jones and Arp (2015) observed catastrophic lake drainage of 0.87 million m<sup>3</sup> of lake water in 36 h on the Alaska Arctic Coastal Plain. Thus, with permafrost degradation, expanding open-talik and better hydraulic connections may dramatically change streamflow features.

Improved hydraulic connections are detected in the SAYR as well. Gao et al. (2019) explored hydrogeological regimes in the periphery area of a thermokarst lake in the south-central SAYR by using electrical resistivity tomography (ERT) and demonstrated that the lake was recharged by the sub-permafrost water. Wan et al. (2019) employed methods of isotope mass balance and time-for-space approach and found an improved hydraulic connection of thermokarst lakes with groundwater from degrading permafrost. Zheng et al. (2016) measured the <sup>222</sup>Rn isotope. It was found that with permafrost degradation, <sup>222</sup>Rn concentration in surface waters turns higher, indicating for an improved hydraulic connectivity.

Although some studies have reported improved hydraulic connections in the SAYR, it is still hard to quantitatively

integrate how much of the sub-permafrost water is discharged and/or recharged to thermokarst lakes, icings, springs and pingos, eventually impacting the YR streamflow. However, GRACE data have proven an increased groundwater storage in many other permafrost basins (e.g., Muskett and Romanovsky, 2011; Guo et al., 2016; Xiang et al., 2016; Xu et al., 2016; Zhang et al., 2017) and a widespread augment in winter flow in northern basins (e.g., Smith et al., 2007; Walvoord and Striegl, 2007; St. Jacques and Sauchyn, 2009; Carey et al., 2012; Walvoord et al., 2012; Lamontagne-Hallé et al., 2018) and on the QTP (Ge et al., 2011; Lan et al., 2015). This indirectly indicates that, under a warming climate and in watersheds of degrading permafrost, the changing discharge to surface waters is of less importance in comparison with the changing recharge to the sub-permafrost water (Table 3).

#### 4.3. Sinkhole-sieve effects of the YR streamflow and permafrost extent

Permafrost, especially ice-rich permafrost, with a low hydraulic conductivity, can substantially restrain rainfall or meltwater from infiltration. In continuous permafrost regions, rainfall is mostly restrained within the seasonally thawed layer (the active layer) and laterally delivered to stream channels. With degrading permafrost, such as that in terms of decreased continuity of permafrost extent, expanded open-talik will

Table 3

Examples of increased groundwater storage in northern basins and on the Qinghai-Tibet Plateau (QTP) underlain by permafrost.

Region	Areal extent (million km <sup>2</sup> )	Permafrost extent (%)	Changes in groundwater storage (billion m <sup>3</sup> )	Evaluation methods	Data period and references
<b>Arctic permafrost regions</b>					
Lena River Basin	2.43	78	26.6 ± 2.3 32 ± 10 44.69 ± 8.36	GRACE	2002–2009 Llovela et al. (2010) 2002–2010 Velicogna et al. (2012) 2008–2008 Muskett and Romanovsky (2009)
Yenisei River Basin	2.4	33	37.75 ± 8.83	GRACE	2002–2008 Muskett and Romanovsky (2009)
Ob River Basin	2.99	1	22.69 ± 8.49	GRACE	2002–2008 Muskett and Romanovsky (2009)
Alaska Arctic coastal plain	0.1	>90%	2.95 ± 1.97	GRACE	2002–2008 Muskett and Romanovsky (2011)
<b>Boreal permafrost regions</b>					
Amur River Basin	1.6 (1.855)		−2.4 ± 2.3	GRACE	2002–2009 Velicogna et al. (2012)
Songhua River Basin	0.54		3.91 ± 1.06	GRACE	1998–2008 Chen et al. (2019)
<b>Alpine and high-plateau permafrost regions</b>					
Qinghai-Tibet Plateau	2.5	42.5	5.01 ± 1.59	GRACE, Landsat MSS, ICESat, TOPEX/POSEIDON, ICESat/GLA14	2003–2014 Zhang et al. (2017)
Qilian Mountains			5.3	GRACE	2003–2012 Guo et al. (2016)
Source area of Nu and Lancang Rivers	0.795		1.77 ± 2.09	Hydro-geodesy, sat gravity & sat altimetry data,	2003–2014 Xiang et al. (2016)
Source area of Yangtze River	1.77–1.81		1.86 ± 1.69	hydrol models & model GIA	Xiang et al. (2016)
Source area of Yellow River	0.1212	86	1.14 ± 1.39		Xiang et al. (2016)
Jinsha River Basin	0.485		2.46 ± 2.24		Xiang et al. (2016)
Qaidam Basin	0.256		1.52 ± 0.95	GRACE	2003–2012 Jiao et al. (2015)
			2.33	GRGS's RL05	2003–2012 Guo et al. (2016)

lessen lateral water delivery and boost vertical infiltration. They can be vividly depicted as sinkhole sieves, altering subsurface and surface hydrological processes and seasonal and inter-annual regimes of streamflow.

In the SAYR, discontinuous and sporadic permafrost presents extensively and they are undergoing substantial degradation. Degrading permafrost in the SAYR will result in sinkhole-sieve effects on streamflow, such as the boosted winter baseflow and lessened summer stormflow. Seasonal trends of streamflow and hydrograph are employed for examining the sinkhole-sieve effects of permafrost degradation on the YR streamflow in the SAYR. Fig. 3 depicts the shifts in seasonal dynamics of YR streamflow in the four sub-basins in the SAYR. The winter streamflow shows consistently increasing trends (grey shades), and summer and autumn streamflow (green and yellow shades, respectively) decline in Sub-basins 1, 2 and 4 with higher permafrost extent (>27%). Sub-basin 3, with a permafrost extent of only 9%, shows declining trends for the YR streamflow as observed in all seasons.

In Fig. 4, five-year average normalized hydrographs are drawn for all sub-basins. With similar trends in seasonal and monthly change precipitation and evaporation, the Sub-basin 1 (HAYR) shows a remarkable and gradually flattened hydrograph. However, in the more downstream Sub-basins 2, 3 and 4, hydrographical changes are not as evident. This well depicts that the sinkhole-sieve effect of degrading permafrost impacts more significantly on the YR streamflow at HHY, shifting the intra-annual regimes of streamflow to the right and flattening the hydrograph.

Basin characteristics, such as low-relief landscapes, organic-rich soils, and well-covered vegetation, can trap and intercept rain- and snow-fall, benefiting vertical infiltration (Davie, 2008). The sinkhole-sieve impact on streamflow changes in regions of degrading permafrost will strengthen under these basin regimes. The Sub-basin 1 with these basin characteristics also help flatten the hydrograph.

## 5. Hydrometeorological and causal analyses for changing YR streamflow in the SAYR

Permafrost degradation has impacted the YR streamflow in the SAYR, especially in the Sub-basin 1. Analysis on change trends for precipitation and evaporation, principal items in regional water budget, is necessary for an integrated perspective of changing YR streamflow in the SAYR. Firstly, the contribution of the annual streamflow at each sub-basin to the YR streamflow in the SAYR and their change trends are analyzed. Then, annual and decadal changes in the YR streamflow are analyzed to detect low-flow periods, which leads to the general downward trend of streamflow, and compared with temperature, precipitation and evaporation. In the end, seasonal changes in precipitation and evaporation are further analyzed for understanding the causes of changes in the YR streamflow.

### 5.1. Inter-annual trends and hydrometeorological contributions to changing YR streamflow

Fig. 5 shows the contribution of YR streamflow from four sub-basins to the SAYR at TNG and their change trends. The HAYR, or Sub-basin 1, underwent significant hydrological impacts from permafrost degradation. However, the streamflow contribution from the HAYR to the YR streamflow at TNG was only 4.09%. Slightly impacted by permafrost degradation, Sub-basins 2, 3 and 4 provided almost all the YR streamflow at the TNG (95.9%). Thus, the declining trend of YR streamflow in the SAYR was resulted mainly from the decreasing streamflow in Sub-basins 2, 3 and 4, particularly in Sub-basin 3 (50.38%).

### 5.2. Inter-annual and decadal changes in YR streamflow

More details of annual and decadal changes in the YR streamflow are illustrated in Fig. 6. Before 1990, annual and decadal streamflows were largely above the multi-year average (black line). During 1990–2010, they went below the average and lasted for almost two decades (rectangle). Around 2010, the YR streamflow went above the black line again, returning to a higher flow. This lasting low-flow period largely accounts for the generally declining trend of the YR streamflow in the SAYR. The decreases of flow depth in four sub-basins were 4.6 mm (HAYR), 9.8 mm (Sub-basin 2), 39.0 mm (Sub-basin 3), and 31.0 mm (Sub-basin 4) in the average YR streamflow. This re-confirms the conclusion that the streamflow decline in the Sub-basin 3 accounts for most of the declined YR streamflow as observed at TNG.

By comparing changes in the streamflow with those in air temperature, precipitation and evaporation, it is evident that the low-flow period (1990–2009) in the SAYR and sub-basins are attributed to persistently increasing evaporation and low precipitation. Since the late 1990s, air temperature has gone upwards much more rapidly (rectangle). This synchronizes with rapidly increasing evaporation, when precipitation stays at a low level. In the mid-2000s, precipitation returned to a high level when evaporation went up persistently to an unprecedented high. Thus, potential evaporation and low precipitation jointly resulted in an extended low-flow period.

In history, three dry-ups of YR flow occurred in the upstream SAYR in 1980, 1988 and 1995, as marked with dash-line rectangles in Fig. 6. The reasons for these three dips in YR discharge have been lively debated. Some suggested reasons for these dry-ups include the FSHS dam construction, permafrost degradation (Qiu, 2012) and hydrometeorological changes (Liang et al., 2010). The dam construction started in 1998, which was later than the earlier years of the YR dry-ups. The impacts of permafrost degradation on the YR streamflow and groundwater table are concluded in Section 3 and regarded as for boosting the YR streamflow. In Fig. 6, the years of YR flow dry-ups concurred in those of high evaporation and low precipitation. The dry-ups in the HAYR should be closely related to spiked evaporation and declined precipitation.



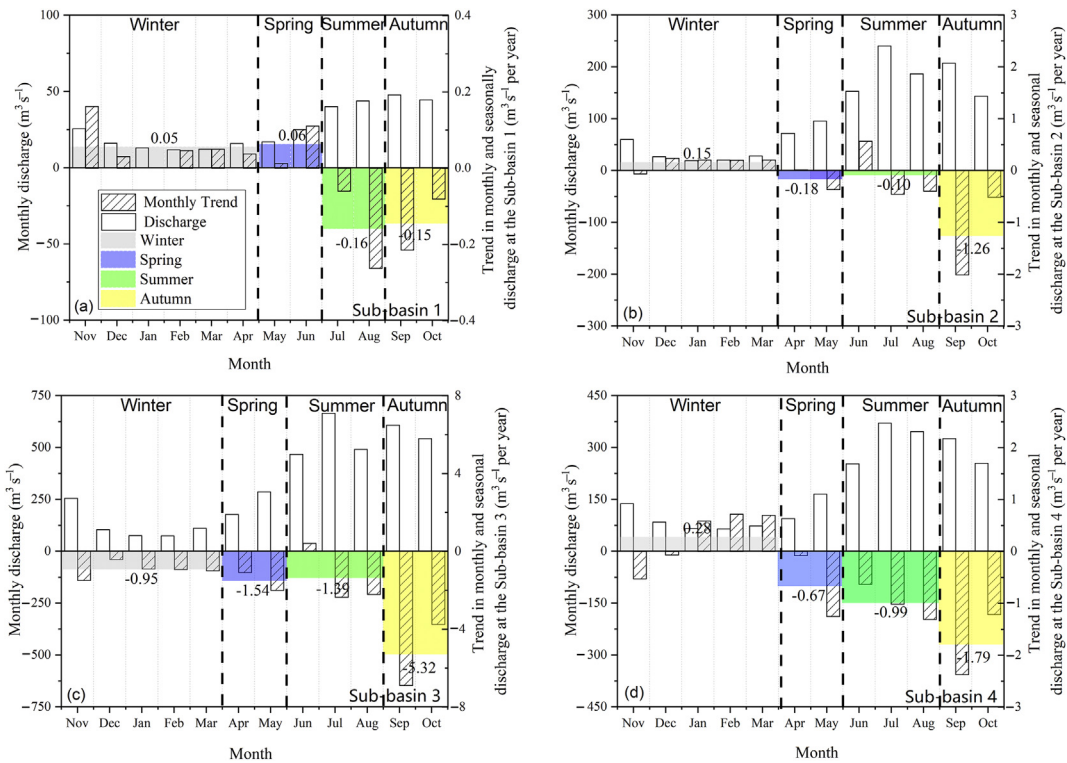


Fig. 3. Trends in monthly and seasonal YR streamflow in the four sub-basins in the SAYR on the northeastern Qinghai-Tibet Plateau during 1961–2017.

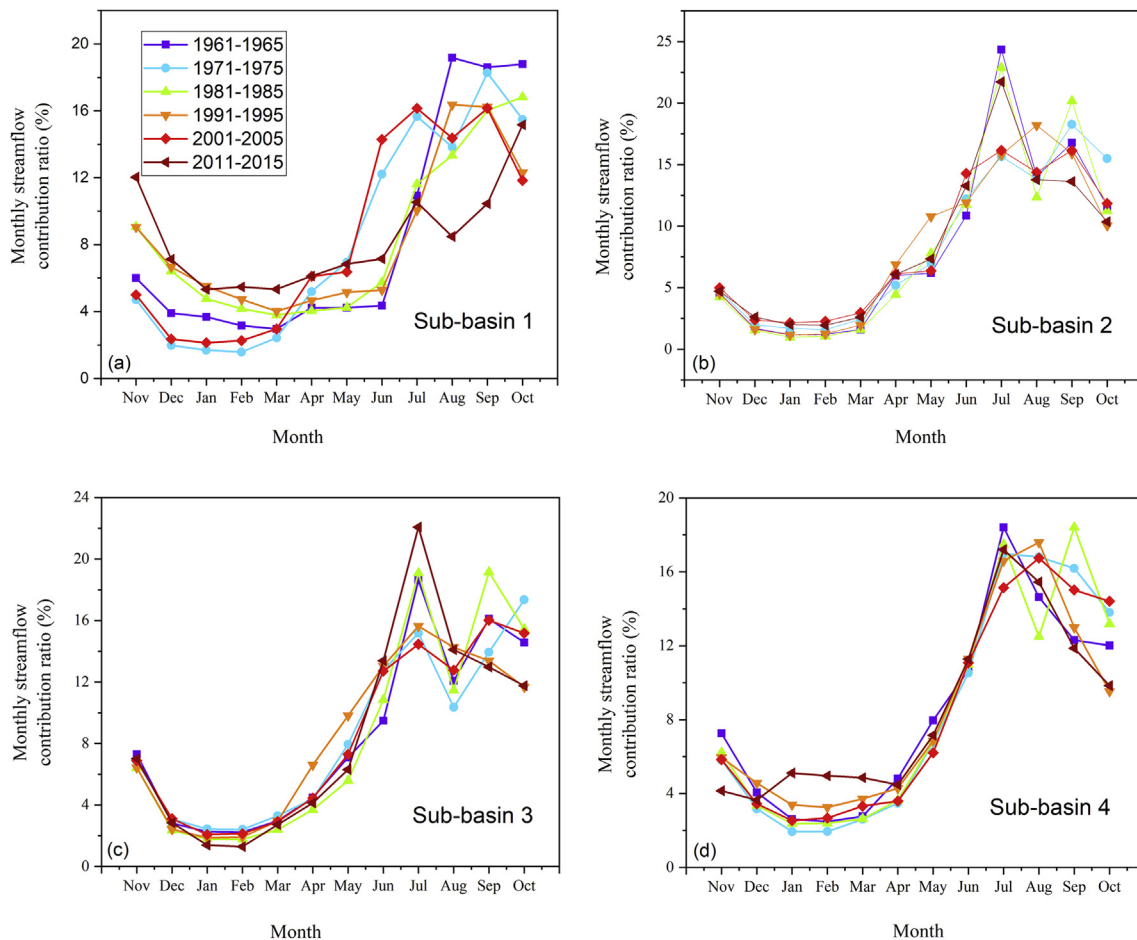


Fig. 4. Seasonal shifts in hydrographs in four sub-basins in the SAYR, northeastern Qinghai-Tibet Plateau.

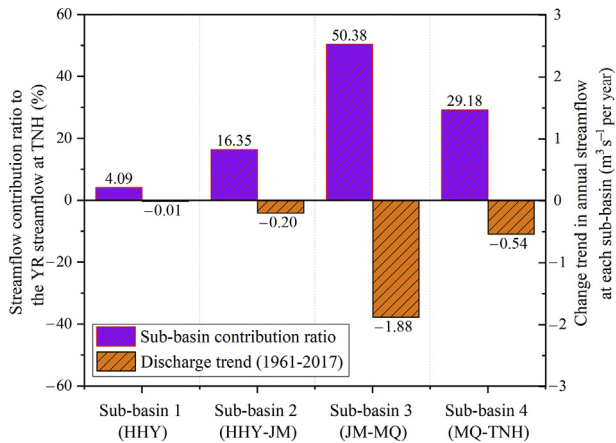


Fig. 5. Trends and contribution of the SAYR to YR streamflow in four sub-basins, northeastern Qinghai-Tibet Plateau during 1961–2017.

5.3. Impacts of changing seasonal distribution in precipitation and evaporation on YR flows

It is now known that the general declining trends of streamflow in the SAYR and sub-basins are attributed to low

precipitation and potent evaporation. What are the reasons for low annual precipitation and strong evaporation? Despite of a general upward trend in annual precipitation, a marked change in seasonal regimes of precipitation was observed in the SAYR during 1961–2017 (Fig. 7): increase in cold seasons (winter and spring) and decline in warm seasons (summer and autumn), especially in August and September, a sign of declining Southwest China Autumn Rain (Bai and Dong, 2004). Evaporation show a significant increase in summer (Fig. 9). In comparison with Fig. 3, the general decline in annual streamflow can be attributed to decreasing streamflow in summer and autumn, probably resulting from declining Southwest China Autumn Rain and significantly enhancing evaporation in summer season.

In the SAYR, precipitation generally synchronizes with air temperature. The increasing precipitation in both the first month of spring and last month in autumn among all sub-basins demonstrate a warmer and wetter climate as a result of an advanced spring and delayed autumn in the SAYR.

In Sub-basin 4, slightly increasing evaporation (Fig. 8) and pronounced increase in precipitation (Fig. 7) in cold season,

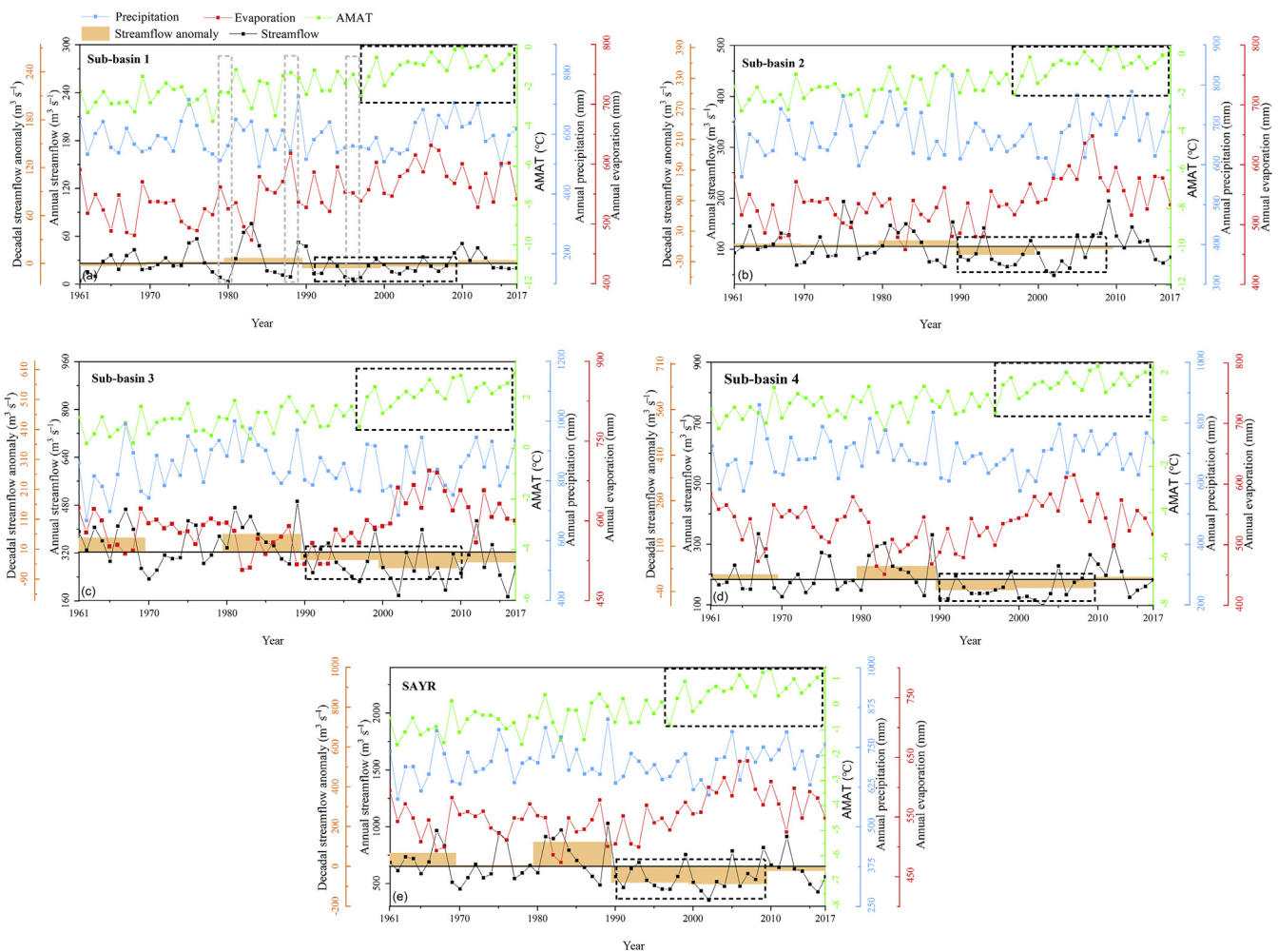


Fig. 6. Changes in the streamflow, evaporation, precipitation and air temperature in the SAYR on northeastern Qinghai-Tibet Plateau (The black line is the average of 1961–2017).

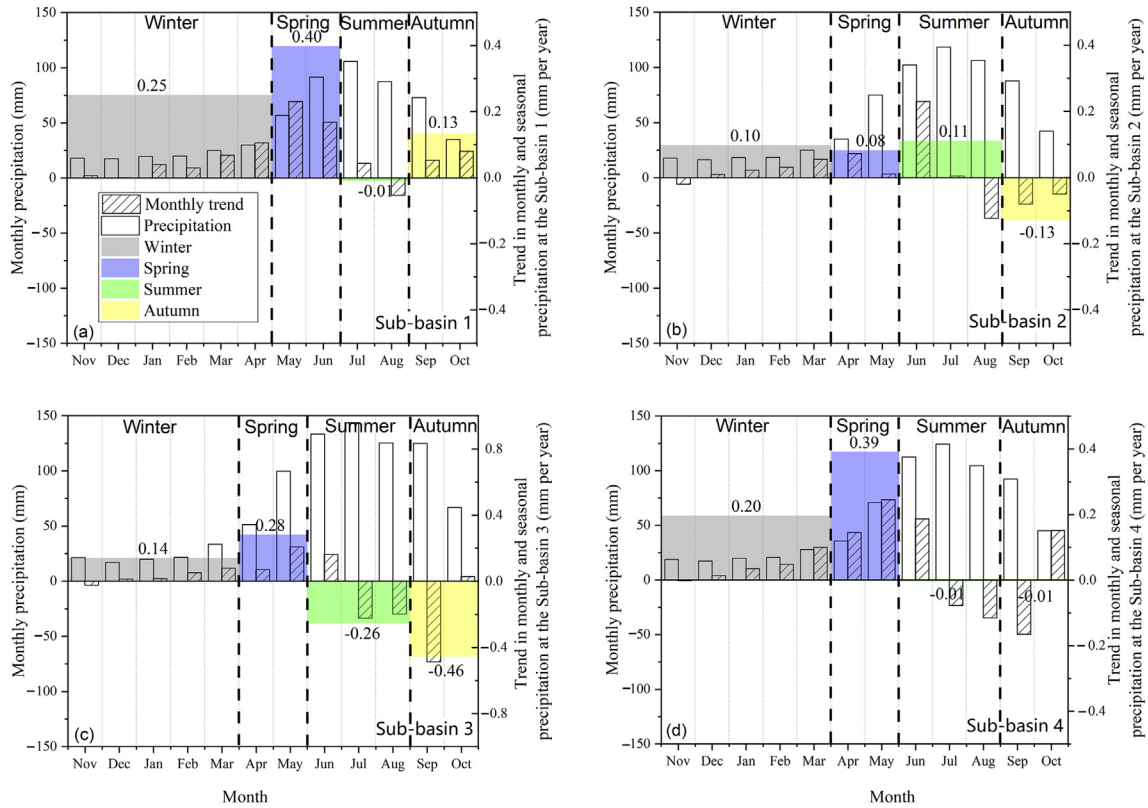


Fig. 7. Trends in monthly and seasonal precipitation in the four sub-basins in the SAYR on northeastern Qinghai-Tibet Plateau during 1961–2017.

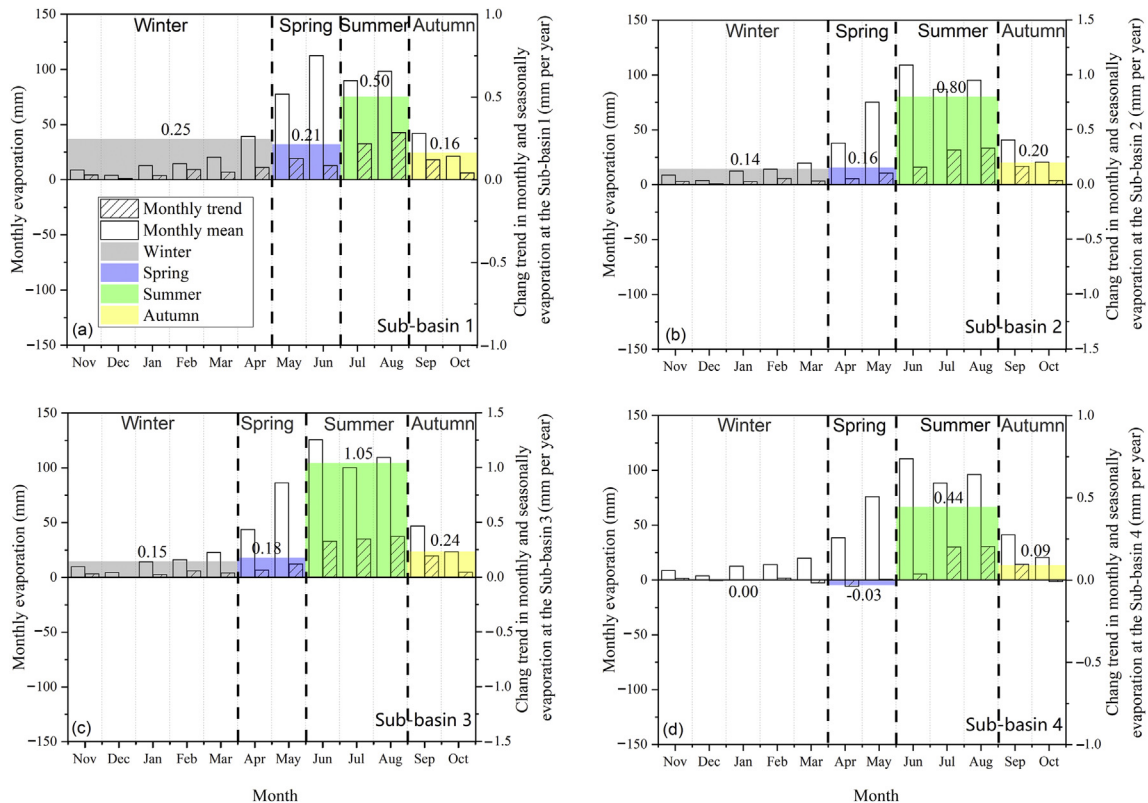


Fig. 8. Trends in monthly and seasonal evaporation in the four sub-basins in the SAYR on northeastern Qinghai-Tibet Plateau during 196–2017.

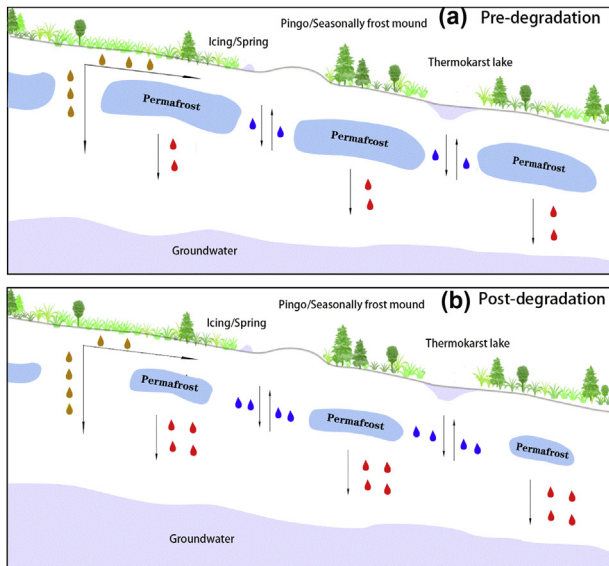


Fig. 9. Conceptual sketch of hydrological shifts on pre-degradation (a) and post-degradation (b) permafrost slopes in the SAYR on the northeastern Qinghai-Tibet Plateau (Red droplet refers to ground-ice-melt water; Blue droplet refers to water delivered by improved hydraulic connectivity, and; Brown droplet refers to water transferred by rainfall infiltration. Droplet number does not proportionally and precisely represent the actual water quantity.).

when surface hydrological processes mostly have paused, are supposed to induce elevated spring streamflow. Unexpectedly, a decreased spring streamflow occurred (Fig. 3). Due to more dams and croplands in the Zoigé Plateau and lower reaches of the SAYR (Hu et al., 2014), the decreased spring YR streamflow in Sub-basins 3 and 4 may not only be driven by the appreciably increased evaporation, but also by anthropogenic disturbances, such as water damming for domestic usage and agricultural irrigation.

#### 5.4. Causal analyses for changing YR streamflow

Some recent research has regarded permafrost degradation as a cause for the SAYR streamflow decrease (e.g., Li et al., 2012; Wang et al., 2018c). The impacts of degrading permafrost on the YR streamflow in the SAYR involve in: 1) ice-melt recharge, 2) discharge of groundwater to pingos and seasonally frost mounds, icings, springs, wetlands and thermokarst lakes, and recharge of thermokarst lakes, and; 3) shifts in seasonal streamflow patterns and flattened hydrographs due to increased vertical infiltration of precipitation (Fig. 9). However, permafrost degradation hardly reduces the YR streamflow; rather, it may enhance the streamflow. Furthermore, the deterioration of vegetation also accelerates permafrost degradation and subsequently results in substantial hydrological impacts. The streamflow contribution ratio of permafrost degradation is 4.09% (in the Sub-basin 1 undergoing substantially hydrological shifts), and; the contribution of ice-melt to streamflow is 0.32% in the Sub-basins 2, 0.12% in the Sub-basin 3, and 0.33% in the Sub-basin 4. A total of 4.9% is quantified as the impacts of degrading permafrost on the YR streamflow in the SAYR.

In August–September, the weakening of the Southwest China Autumn Rain and significantly increasing evaporation in summer are the major reasons for general downward trend of YR streamflow in the SAYR, especially in main streamflow contribution sub-basins (i.e., Sub-basins 3 and 4). Anthropogenic disturbances tend to reduce the YR streamflow in the SAYR.

#### 5.5. Uncertainty analyses

A value of 4.09% (streamflow contribution of the HAYR to the SYAR flow at TNG), taken as a partially quantified hydrological impact of permafrost degradation in the HAYR, may be overestimated. Even though, the HAYR, with minimal anthropogenic disturbances, undergoes substantially hydrological shifts as a result of permafrost degradation.

The ice-melt water for recharging groundwater and YR streamflow among sub-basins and in the SAYR remains uncertain due to inadequate data for runoff generation and outflowing pathways, as well as the projected timespan for permafrost thaw, such as the 100 years projection under the RCP 4.5 scenario. Meanwhile, evaluation of improved hydraulic connectivity in Sub-basins 2, 3 and 4 is largely neglected due to the scarcity of relevant data. Nonetheless, 4.9% is a still referable value based on current recognition of mechanisms for the hydrological impacts of permafrost degradation on the YR streamflow.

## 6. Conclusions and prospects

### 6.1. Summaries

- 1) Hydrological impacts on the YR streamflow from degrading permafrost in the SAYR can be divided into three major parts:
  - i. Ice-melt will recharge groundwater storage. The ice-melt recharge accounts for 14.4% of annual streamflow in Sub-basin 1 (HAYR); 1.9% in Sub-basin 2; 0.2% in Sub-basin 3; 1.1% in Sub-basin 4; and overall, an average of 1.3% over the SAYR.
  - ii. Improved hydraulic connections boost hydrothermal exchanges between surface waters and sub-permafrost waters. Widely detected increase in winter flow in the SAYR suggests more discharge of the sub-permafrost water to surface waters.
  - iii. Sinkhole-sieve mechanisms of permafrost degradation on surface flows will redistribute streamflow, boost vertical infiltration, reduce lateral delivery, and alter intra-annual distribution of YR streamflow. However, sinkhole-sieve mechanism is merely detected in Sub-basin 1 (HAYR).
- 2) Permafrost degradation has only appreciable impacts on the YR streamflow in the SAYR (4.9%). Declined Southwest China Autumn Rain and enhanced summer evaporation may largely account for the declined SAYR streamflow. Overgrazing, damming and irrigation might have also contributed to the declined YR streamflow to certain extents. Under a warming climate, advance of

spring and delay of autumn may help boost the YR streamflow in the first month in spring and last month in autumn in the SAYR as a whole.

## 6.2. Inadequacies

In the aspects of data availability hydrometeorological and geocryological data are still inadequate to fully substantiate the impacts of permafrost degradation on changes in the YR streamflow. Subsurface geological structures and vertical and lateral extents and ice content of permafrost, as well as hydrothermal parameters of varied soil types in frozen/unfrozen conditions, are insufficiently investigated in the SAYR. These result in difficulties in modeling dynamics of permafrost changes, ground-ice melt-water recharge to groundwater, and subsurface hydrological processes in the environment of degrading permafrost under a warming climate. Monitoring of changes in hydrothermally-influenced landscapes, soil ice-content in the active layer and implement of isotope tracing techniques are still inadequate in the SAYR. Long-term hydrometeorological observations, change in thermally-influenced landscapes, vertical and lateral permafrost extent, ice-content and subsurface geological structures are key to bolstering the pertinent understanding and how the streamflow would change under a warming climate in the future.

## 6.3. Prospects

Multi-scale and multi-method approaches are required to study the impacts of permafrost degradation on the SAYR streamflow. Remote sensing techniques/unmanned aerial vehicles in combination with geophysical methods can be employed to feature vertical and lateral extent of permafrost and ice-content of permafrost and subsurface geological structures. Field investigations for surface waters and landscape types, *in-situ* hydrothermal dynamics and borehole observations and sampling, should be incorporated. Laboratory analyses of hydrothermal parameters and other soil properties associated with freeze/thaw cycles, especially for varied saturation conditions, are also important. Long-term hydrometeorological observations and chemical/isotopic tracing techniques integrating numerical simulations can better constrain the hydrological impacts of permafrost degradation in the SAYR. Among the above-mentioned methods, remote sensing techniques for basin-scale spontaneous observations and isotope-tracing techniques should be prioritized.

## Conflict of interest

The authors declare no conflict of interest.

## Acknowledgments

This work was supported by the Chinese Academy of Sciences Strategic Priority Research Program (XDA20100103), Ministry of Science and Technology of

China Key R&D Program (2017YFC0405704), and CAS Overseas Professorships of Victor F Bense and Sergey S Marchenko at the former Cold and Arid Regions Environmental and Engineering Research Institute (now renamed to Northwest Institute of Eco-Environment and Resources), CAS during 2013–2016.

## References

- Bai, H., Dong, W., 2004. Climate features and formation causes of autumn rain over Southwest China. *Plateau Meteorol.* 23 (6), 884–889 (in Chinese).
- Blue, B., Brierley, G., Yu, G., 2013. Geodiversity in the Yellow River source zone. *J. Geogr. Sci.* 23 (5), 775–792. <https://doi.org/10.1007/s11442-013-1044-4>.
- Bring, A., Destouni, G., 2014. Arctic climate and water change: model and observation relevance for assessment and adaptation. *Surv. Geophys.* 35, 853–877. <https://doi.org/10.1007/s10712-013-9267-6>.
- Bring, A., Fedorova, I., Dibike, Y., et al., 2016. Arctic terrestrial hydrology: a synthesis of processes, regional effects, and research challenges. *J. Geophys. Res. Biogeosci.* 121, 621–649. <https://doi.org/10.1002/2015JG003131>.
- Bring, A., Shiklomanov, A., Lammers, R.B., 2017. Pan-Arctic river discharge: prioritizing monitoring of future climate change hot spots. *Earth's Future* 5 (1), 72–92. <https://doi.org/10.1002/2016ef000434>.
- Brown, J., Ferrians, O., Heginbottom, J.A., et al., 2002. *Circum-Arctic Map of Permafrost and Ground-Ice Conditions. Version 2.* Boulder, Colorado USA.
- Carey, S.K., Woo, M., 2001a. Spatial variability of hillslope water balance, wolf creek basin, subarctic Yukon. *Hydrol. Process.* 15 (16), 3113–3132. <https://doi.org/10.1002/hyp.319>.
- Carey, S.K., Woo, M.K., 2001b. Slope runoff processes and flow generation in a subarctic, subalpine catchment. *J. Hydrol.* 253 (1–4), 110–129. [https://doi.org/10.1016/S0022-1694\(01\)00478-4](https://doi.org/10.1016/S0022-1694(01)00478-4).
- Carey, S.K., Boucher, J.L., Duarte, C.M., 2012. Inferring groundwater contributions and pathways to streamflow during snowmelt over multiple years in a discontinuous permafrost subarctic environment (Yukon, Canada). *Hydrogeol. J.* 21 (1), 67–77. <https://doi.org/10.1007/s10040-012-0920-9>.
- Chen, H., Zhang, W.C., Nie, N., et al., 2019. Long-term groundwater storage variations estimated in the Songhua River Basin by using GRACE products, land surface models, and in-situ observations. *Sci. Total Environ.* 649, 372–387. <https://doi.org/10.1016/j.scitotenv.2018.08.352>.
- Cheng, G.D., Zhao, L., Li, R., et al., 2019. Characteristics, changes and impacts of permafrost on Qinghai-Tibet Plateau. *Chin. Sci. Bull.* 64 (27), 2783–2795 (in Chinese).
- CMWR (Chinese Ministry of Water Resources), 2008–2017. China river sediment bulletin. <http://www.mwr.gov.cn/sj> (in Chinese).
- Davie, T., 2008. *Fundamentals of Hydrology.* Routledge.
- Fritz, M., Opel, T., Tanski, G., et al., 2015. Dissolved organic carbon (DOC) in Arctic ground ice. *Cryosphere* 9 (2), 737–752. <https://doi.org/10.5194/tc-9-737-2015>.
- Gao, B., Yang, D., Qin, Y., et al., 2018. Change in frozen soils and its effect on regional hydrology, upper Heihe basin, northeastern Qinghai-Tibetan Plateau. *Cryosphere* 12 (2), 657. <https://doi.org/10.5194/tc-12-657-2018>.
- Gao, S., Jin, H., Bense, V.F., et al., 2019. Application of electrical resistivity tomography for delineating permafrost hydrogeology in the headwater area of Yellow River on Qinghai-Tibet Plateau, SW China. *Hydrogeol. J.* 27 (5), 1725–1737. <https://doi.org/10.1007/s10040-019-01942-z>.
- Ge, S., Yang, D., Kane, D.L., 2013. Yukon River Basin long-term (1977–2006) hydrologic and climatic analysis. *Hydrol. Process.* 27 (17), 2475–2484. <https://doi.org/10.1002/hyp.9282>.
- Ge, S., McKenzie, J., Voss, C., et al., 2011. Exchange of groundwater and surface-water mediated by permafrost response to seasonal and long term air temperature variation. *Geophys. Res. Lett.* 38 (14), L14402. <https://doi.org/10.1029/2011gl047911>.
- Guo, J.Y., Mu, D.P., Liu, X., et al., 2016. Water storage changes over the Tibetan Plateau revealed by GRACE mission. *Acta Geophys.* 64, 463–476. <https://doi.org/10.1515/acgeo-2016-0003>.

- Haine, T.W.N., Curry, B., Gerdes, R., et al., 2015. Arctic freshwater export: status, mechanisms, and prospects. *Global Planet. Change* 125, 13–35. <https://doi.org/10.1016/j.gloplacha.2014.11.013>.
- Han, T., Pu, H., Cheng, P., et al., 2016. Hydrological effects of alpine permafrost in the headwaters of the Urumqi river, Tianshan mountains. *Sci Cold Arid Reg.* 8 (3), 241–249. <https://doi.org/10.3724/SP.J.1226.2016.00241>.
- Hu, G., Jin, H., Dong, Z., et al., 2014. Research of land-use and land-cover change (LUCC) in the source regions of the Yellow River. *J. Glaciol. Geocryol.* 36 (3), 573–581. <https://doi.org/10.7522/j.issn.1000-0240.2014.0068> (in Chinese).
- IPCC, 2013. *Climate Change 2013: The Physical Science Basis. Contribution of Working Group I to the Fifth Assessment Report of the Intergovernmental Panel on Climate Change.* Cambridge University Press, Cambridge and New York.
- Jiao, J.J., Zhang, X., Liu, Y., et al., 2015. Increased water storage in the Qaidam basin, the north Tibet Plateau from GRACE gravity data. *PLoS One* 10 (10), e0141442. <https://doi.org/10.1371/journal.pone.0141442>.
- Jin, H.J., He, R.X., Cheng, G.D., et al., 2009. Changes in frozen ground in the source area of the Yellow River on the Qinghai–Tibet Plateau, China, and their eco-environmental impacts. *Environ. Res. Lett.* 4, 045206 <https://doi.org/10.1088/1748-9326/4/4/045206>.
- Jin, H.J., Wang, Q.F., Che, T., et al., 2019. Assessment report on impacts of glacier retreat and permafrost thaw on the alpine ecosystems and surface runoffs in the upper Yellow River Basin.
- Jones, B.M., Arp, C.D., 2015. Observing a catastrophic thermokarst lake drainage in northern Alaska. *Permafr. Periglac.* 26 (2), 119–128. <https://doi.org/10.1002/ppp.1842>.
- Kane, D.L., Yoshikawa, K., McNamara, J.P., 2013. Regional groundwater flow in an area mapped as continuous permafrost, NE Alaska (USA). *Hydrogeol. J.* 21, 41–52. <https://doi.org/10.1007/s10040-012-0937-0>.
- Kokelj, S.V., Lacelle, D., Lantz, T.C., et al., 2013. Thawing of massive ground ice in mega slumps drives increases in stream sediment and solute flux across a range of watershed scales. *J. Geophys. Res. Earth* 118 (2), 681–692. <https://doi.org/10.1002/jgrf.20063>.
- Kurylyk, B.L., Hayashi, M., Quinton, W.L., et al., 2016. Influence of vertical and lateral heat transfer on permafrost thaw, peatland landscape transition, and groundwater flow. *Water Resour. Res.* 52, 1286–1305. <https://doi.org/10.1002/2015WR018057>.
- Lamontagne-Hallé, P., McKenzie, J.M., Kurylyk, B.L., et al., 2018. Changing groundwater discharge dynamics in permafrost regions. *Environ. Res. Lett.* 13 (8), 084017 <https://doi.org/10.1088/1748-9326/aad404>.
- Lan, C., Zhang, Y., Bohn, T.J., et al., 2015. Frozen soil degradation and its effects on surface hydrology in the northern Tibetan Plateau. *J. Geophys. Res. Atmos.* 120, 8276–8298. <https://doi.org/10.1002/2015JD023193>.
- Li, L., Shen, H., Dai, S., et al., 2012. Response of runoff to climate change and its future tendency in the source region of Yellow River. *J. Geogr. Sci.* 22 (3), 431–440. <https://doi.org/10.1007/s11442-012-0937-y>.
- Liang, S., Ge, S., Wan, L., et al., 2010. Can climate change cause the Yellow River dry up? *J. Hydrol.* 46, W02505. <https://doi.org/10.1029/2009WR007971>.
- Llovela, W., Beckera, M., Cazenave, A., et al., 2010. Global land water storage change from GRACE over 2002–2009; Inference on sea level. *Compt. Rendus Geosci.* 342, 179–188. <https://doi.org/10.1016/j.crte.2009.12.004>.
- Luo, D., Jin, H., Wu, Q., et al., 2018. Thermal regime of warm-dry permafrost in relation to ground surface temperature in the Source Areas of the Yangtze and Yellow Rivers on the Qinghai–Tibet Plateau, SW China. *Sci. Total Environ.* 618, 1033–1045. <https://doi.org/10.1016/j.scitotenv.2017.09.083>.
- Lutgens, F.K., Tarbuck, E.J., 2012. *Essentials of geology. Crustal Deformation and Mountain Building.* Prentice Hall.
- Muskett, R., Romanovsky, V., 2009. Groundwater storage changes in arctic permafrost watersheds from GRACE and in situ measurements. *Environ. Res. Lett.* 4 (4), 045009 <https://doi.org/10.1088/1748-9326/4/4/045009>.
- Muskett, R., Romanovsky, V., 2011. Alaskan permafrost groundwater storage changes derived from GRACE and ground measurements. *Rem. Sens.* 3 (2), 378–397. <https://doi.org/10.3390/rs3020378>.
- Neff, J.C., Finlay, J.C., Zimov, S.A., et al., 2006. Seasonal changes in the age and structure of dissolved organic carbon in Siberian rivers and streams. *Geophys. Res. Lett.* 33 (23), L23401. <https://doi.org/10.1029/2006gl028222>.
- Niu, L., Ye, B., Ding, Y., et al., 2016. Response of hydrological processes to permafrost degradation from 1980 to 2009 in the upper Yellow River basin, China. *Nord. Hydrol.* 47 (5), 1014–1024. <https://doi.org/10.2166/nh.2016.096>.
- O'Donnell, J.A., Aiken, G.R., Swanson, D.K., et al., 2016. Dissolved organic matter composition of Arctic rivers: linking permafrost and parent material to riverine carbon. *Global Biogeochem. Cycles* 30 (12), 1811–1826. <https://doi.org/10.1002/2016gb005482>.
- Qin, Y., Yang, D., Gao, B., et al., 2017. Impacts of climate warming on the frozen ground and eco-hydrology in the Yellow River source region, China. *Sci. Total Environ.* 605–606, 830–841. <https://doi.org/10.1016/j.scitotenv.2017.06.188>.
- Qiu, J., 2012. Thawing permafrost reduces river runoff. *Nature.* <https://doi.org/10.1038/nature.2012.9749>.
- Ran, Y., Li, X., Cheng, G., et al., 2012. Distribution of permafrost in China: an overview of existing permafrost maps. *Permafr. Periglac.* 23, 322–333. <https://doi.org/10.1002/ppp.1756>.
- Scheidegger, J.M., 2013. *Impact of permafrost dynamics on Arctic groundwater flow systems with application to the evolution of spring and lake taliks.* University of East Anglia, Norwich.
- Searcy, J.K., Hardison, C.H., 1960. *Double-mass curves.* U. S. Geological Survey, Washington, D. C.
- Smith, L.C., Pavelsky, T.M., MacDonald, G.M., et al., 2007. Rising minimum daily flows in northern Eurasian rivers: a growing influence of groundwater in the high-latitude hydrologic cycle. *J. Geophys. Res. Biogeo.* 112, G04S47. <https://doi.org/10.1029/2006JG000327>.
- St Jacques, J.M., Sauchyn, D.J., 2009. Increasing winter baseflow and mean annual streamflow from possible permafrost thawing in the Northwest Territories, Canada. *Geophys. Res. Lett.* 36 (1), L01401. <https://doi.org/10.1029/2008gl035822>.
- Takeuchi, K., Kundzewicz, Z.W., Rosbjerg, D., et al., 2004. *Northern Research Basins Water Balance.* Centre for Ecology and Hydrology. IAHS Press, Wallingford, Oxfordshire.
- Velicogna, I., Tong, J., Zhang, T., et al., 2012. Increasing subsurface water storage in discontinuous permafrost areas of the Lena River basin, Eurasia, detected from GRACE. *Geophys. Res. Lett.* 39, L09403. <https://doi.org/10.1029/2012GL051623>.
- Walvoord, M.A., Striegl, R.G., 2007. Increased groundwater to stream discharge from permafrost thawing in the Yukon River basin: potential impacts on lateral export of carbon and nitrogen. *Geophys. Res. Lett.* 34 (12), L12402. <https://doi.org/10.1029/2007gl030216>.
- Walvoord, M.A., Voss, C.I., Wellman, T.P., 2012. Influence of permafrost distribution on groundwater flow in the context of climate-driven permafrost thaw: example from Yukon Flats Basin, Alaska, United States. *Water Resour. Res.* 48, W07524. <https://doi.org/10.1029/2011WR011595>.
- Wan, C., Gibson, J.J., Shen, S., et al., 2019. Using stable isotopes paired with tritium analysis to assess thermokarst lake water balances in the Source Area of the Yellow River, northeastern Qinghai–Tibet Plateau, China. *Sci. Total Environ.* 689, 1276–1292. <https://doi.org/10.1016/j.scitotenv.2019.06.427>.
- Wang, B.L., French, H.M., 1994. Climate controls and high-altitude permafrost, Qinghai–Xizang (Tibet) plateau, China. *Permafr. Periglac.* 5, 87–100. <https://doi.org/10.1002/ppp.3430050203>.
- Wang, B.L., French, H.M., 1995. Permafrost on the Tibet Plateau, China. *Quat. Sci. Rev.* 14, 255–274. [https://doi.org/10.1016/0277-3791\(95\)00006-B](https://doi.org/10.1016/0277-3791(95)00006-B).
- Wang, S.T., Sheng, Y., Li, J., et al., 2018a. An estimation of ground ice volumes in permafrost layers in Northeastern Qinghai–Tibet Plateau, China. *Chin. Geogr. Sci.* 28 (1), 61–73. <https://doi.org/10.1007/s11769-018-0932-z>.
- Wang, T.H., Yang, D.W., Qin, Y., et al., 2018b. Historical and future changes of frozen ground in the upper Yellow River Basin. *Global Planet. Change* 162, 199–211. <https://doi.org/10.1016/j.gloplacha.2018.01.009>.
- Wang, T.H., Yang, H.B., Yang, D.W., et al., 2018c. Quantifying the streamflow response to frozen ground degradation in the source region of the Yellow

- River within the Budyko framework. *J. Hydrol.* 558, 301–313. <https://doi.org/10.1016/j.jhydrol.2018.01.050>.
- Wang, X.Q., Chen, R.S., Yang, Y., 2017. Effects of permafrost degradation on the hydrological regime in the source regions of the Yangtze and Yellow Rivers, China. *Water* 9, 897. <https://doi.org/10.3390/w9110897>.
- Wang, Y., Yang, H., Gao, B., et al., 2018d. Frozen ground degradation may reduce future runoff in the headwaters of an inland river on the north-eastern Tibetan Plateau. *J. Hydrol.* 564, 1153–1164. <https://doi.org/10.1016/j.jhydrol.2018.07.078>.
- Woo, M.K., 2000. McMaster river and arctic hydrology. *Phys. Geogr.* 21 (5), 466–484. <https://doi.org/10.1080/02723646.2000.10642721>.
- Woo, M. k., 2012. *Permafrost Hydrology*. Springer Science & Business Media.
- Wu, P., Liang, S., Wang, X.S., et al., 2018. A new assessment of hydrological change in the Source Region of the Yellow River. *Water* 10, 877. <https://doi.org/10.3390/w10070877>.
- Xiang, L., Wang, H., Steffen, H., et al., 2016. Groundwater storage changes in the Tibetan Plateau and adjacent areas revealed from GRACE satellite gravity data. *Earth Planet Sci. Lett.* 449, 228–239. <https://doi.org/10.1016/j.epsl.2016.06.002>.
- Xu, M., Ye, B.S., Zhao, Q.D., et al., 2013. Estimation of water balance in the source region of the Yellow River based on GRACE satellite data. *J. Arid Land* 5 (3), 384–395. <https://doi.org/10.1007/s40333-013-0169-8>.
- Xu, M., Kang, S., Zhao, Q., et al., 2016. Terrestrial water storage changes of permafrost in the Three-River source region of the Tibetan Plateau, China. *Adv. Meteorol.* 1, 1–13. <https://doi.org/10.1155/2016/4364738>.
- Xu, R., Hu, H.C., Tian, F.Q., et al., 2019. Projected climate change impacts on future streamflow of the Yarlung Tsangpo-Brahmaputra River. *Global Planet. Change* 175, 144–159. <https://doi.org/10.1016/j.gloplacha.2019.01.012>.
- Yang, D., Kane, D., Zhang, Z., et al., 2005. Bias corrections of long-term (1973-2004) daily precipitation data over the northern regions. *Geophys. Res. Lett.* 32, L19501. <https://doi.org/10.1029/2005GL024057>.
- Yang, D., Zhao, Y., Armstrong, R., et al., 2009. Yukon River streamflow response to seasonal snow cover changes. *Hydrol. Process.* 23 (1), 109–121. <https://doi.org/10.1002/hyp.7216>.
- Ye, B.S., Yang, D.Q., Ding, Y.J., et al., 2004. A bias-corrected precipitation climatology for China. *J. Hydrometeorol.* 5, 1147–1160. <https://doi.org/10.1175/JHM-366.1>.
- Ye, B., Yang, D., Zhang, Z., et al., 2009. Variation of hydrological regime with permafrost coverage over Lena Basin in Siberia. *J. Geophys. Res.* 114, D07102. <https://doi.org/10.1029/2008jd010537>.
- Ye, B.S., Ding, Y.J., Jiao, K.Q., et al., 2012. The response of river discharge to climate warming in cold region over China. *Quart. Sci.* 32, 103–110 (in Chinese).
- Zhang, G., Yao, T., Shum, C.K., et al., 2017. Lake volume and groundwater storage variations in Tibetan Plateau's endorheic basin. *Geophys. Res. Lett.* 44 (11), 5550–5560. <https://doi.org/10.1002/2017gl073773>.
- Zhang, S.F., Jia, S.F., Liu, C.M., et al., 2004. Study on the changes of water cycle and its impacts in the source region of the Yellow River. *Sci. China Ser. E* 47, 142–151. <https://doi.org/10.1360/04ez0012>.
- Zheng, G., Yang, Y., Yang, D., et al., 2019. Satellite-based simulation of soil freezing/thawing processes in the northeast Tibetan Plateau. *Remote Sen. Environ. Times* 231, 111269. <https://doi.org/10.1016/j.rse.2019.111269>.
- Zheng, M.J., Wan, C.W., Du, M.D., et al., 2016. Application of Rn-222 isotope for the interaction between surface water and groundwater in the Source Area of the Yellow River. *Nord. Hydrol* 47 (6), 1253–1262. <https://doi.org/10.2166/nh.2016.070>.